

Edith Cowan University  
**Research Online**

---

ECU Publications Pre. 2011

---

2009

## Tunable multi-wavelength fiber lasers based on an Opto-VLSI processor and optical amplifiers

Feng Xiao  
*Edith Cowan University*

Kamal Alameh  
*Edith Cowan University*

Yong Lee  
*Edith Cowan University*

Follow this and additional works at: <https://ro.ecu.edu.au/ecuworks>

 Part of the [Engineering Commons](#)

---

This paper was published in Optics Express and is made available as an electronic reprint with the permission of OSA. The paper can be found at the following URL on the OSA website: <http://www.opticsinfobase.org/abstract.cfm?URI=oe-17-25-23123>. Systematic or multiple reproduction or distribution to multiple locations via electronic or other means is prohibited and is subject to penalties under law.

This Journal Article is posted at Research Online.  
<https://ro.ecu.edu.au/ecuworks/569>

# Tunable multi-wavelength fiber lasers based on an Opto-VLSI processor and optical amplifiers

Feng Xiao<sup>1</sup>, Kamal Alameh<sup>1,\*</sup>, and Yong Tak Lee<sup>2</sup>

<sup>1</sup>WA Center of Excellence for MicroPhotonic System, Electron Science Research Institute, Edith Cowan University, Joondalup, WA, 6027, Australia.

<sup>2</sup>Gwangju Institute of Science and Technology, Department of Information and Communication, Gwangju 500-712, Korea.

\*k.alameh@ecu.edu.au

**Abstract:** A multi-wavelength tunable fiber laser based on the use of an Opto-VLSI processor in conjunction with different optical amplifiers is proposed and experimentally demonstrated. The Opto-VLSI processor can simultaneously select any part of the gain spectrum from each optical amplifier into its associated fiber ring, leading to a multiport tunable fiber laser source. We experimentally demonstrate a 3-port tunable fiber laser source, where each output wavelength of each port can independently be tuned within the C-band with a wavelength step of about 0.05nm. Experimental results demonstrate a laser linewidth as narrow as 0.05 nm and an optical side-mode-suppression-ratio (SMSR) of about 35 dB. The demonstrated three fiber lasers have excellent stability at room temperature and output power uniformity less than 0.5 dB over the whole C-band.

©2009 Optical Society of America

**OCIS codes:** (060.0060) Fiber optics and optical communications; (060.2320) Fiber optics amplifiers and oscillators.

---

## References and links

1. A. Bellemare, "Continuous-wave silica-based erbium-doped fiber lasers," *Prog. Quantum Electron.* **27**(4), 211–266 (2003).
2. M. A. Umyy, N. Madamopoulos, P. Lama, and R. Dorsinville, "Dual Sagnac loop mirror SOA-based widely tunable dual-output port fiber laser," *Opt. Express* **17**(17), 14495–14501 (2009).
3. Q. Wang, Y. Wang, W. Zhang, X. Feng, X. M. Liu, and B. K. Zhou, "Inhomogeneous loss mechanism in multiwavelength fiber Raman ring lasers," *Opt. Lett.* **30**(9), 952–954 (2005).
4. S. Yamashita, and K. Hotate, "Multiwavelength erbium-doped fibre laser using intracavity etalon and cooled by liquid nitrogen," *Electron. Lett.* **32**(14), 1298–1299 (1996).
5. A. Bellemare, M. Karasek, M. Rochette, S. LaRochelle, and M. Tetu, "Room temperature multifrequency erbium-doped fiber lasers anchored on the ITU frequency grid," *J. Lightwave Technol.* **18**(6), 825–831 (2000).
6. J. Yao, J. P. Yao, Z. C. Deng, and J. Liu, "Investigation of room-temperature multiwavelength fiber-ring laser that incorporates an SOA-based phase modulator in the laser cavity," *J. Lightwave Technol.* **23**(8), 2484–2490 (2005).
7. P. C. Peng, K. M. Feng, C. C. Chang, H. Y. Chiou, J. H. Chen, M. F. Huang, H. C. Chien, and S. Chi, "Multiwavelength fiber laser using S-band erbium-doped fiber amplifier and semiconductor optical amplifier," *Opt. Commun.* **259**(1), 200–203 (2006).
8. S. Qin, D. Chen, Y. B. Tang, and S. L. He, "Stable and uniform multi-wavelength fiber laser based on hybrid Raman and Erbium-doped fiber gains," *Opt. Express* **14**(22), 10522–10527 (2006).
9. V. Roy, M. Piché, F. Babin, and G. W. Schinn, "Nonlinear wave mixing in a multilongitudinal-mode erbium-doped fiber laser," *Opt. Express* **13**(18), 6791–6797 (2005).
10. S. L. Pan, C. Y. Lou, and Y. Z. Gao, "Multiwavelength erbium-doped fiber laser based on inhomogeneous loss mechanism by use of a highly nonlinear fiber and a Fabry-Perot filter," *Opt. Express* **14**(3), 1113–1118 (2006).
11. Y. Liu, X. Feng, S. Yuan, G. Kai, X. Dong, "Simultaneous four-wavelength lasing oscillations in an erbium-doped fiber laser with two high birefringence fiber Bragg gratings," *Opt. Express* **12**(10), 2056–2061 (2004).
12. D. S. Moon, U. C. Paek, and Y. Chung, "Polarization controlled multi-wavelength Er-doped fiber laser using fiber Bragg grating written in few-mode side-hole fiber with an elliptical core," *Opt. Express* **13**(14), 5574–5579 (2005).
13. T. Miyazaki, N. Edagawa, S. Yamamoto, and S. Akiba, "A multiwavelength fiber ring-laser employing a pair of silica-based array-waveguide-gratings," *IEEE Photon. Technol. Lett.* **9**(7), 910–912 (1997).
14. M. Zimgib, C. H. Joyner, C. R. Doerr, L. W. Stultz, and H. M. Presby, "An 18-channel multifrequency laser," *IEEE Photon. Technol. Lett.* **8**(7), 870–872 (1996).

15. F. Xiao, B. Juswardy, K. Alameh, and Y. T. Lee, "Novel broadband reconfigurable optical add-drop multiplexer employing custom fiber arrays and Opto-VLSI processors," *Opt. Express* **16**(16), 11703–11708 (2008).
  16. I. G. Manolis, T. D. Wilkinson, M. M. Redmond, and W. A. Crossland, "Reconfigurable multilevel phase holograms for Optical switches," *IEEE Photon. Technol. Lett.* **14**(6), 801–803 (2002).
  17. A. Bellemare, M. Karasek, C. Riviere, F. Babin, G. He, V. Roy, and G. W. Schinn, "A broadly tunable Erbium-doped fiber ring laser: experimentation and modeling," *IEEE J. Sel. Top. Quantum Electron.* **7**(1), 22–29 (2001).
  18. P. F. McManamon, T. A. Dorschner, D. L. Corkum, L. J. Friedman, D. S. Hobbs, M. Holz, S. Liberman, H. Q. Nguyen, D. P. Resler, R. C. Sharp, and E. A. Watson, "Optical phased array technology," *Proc. IEEE* **84**(2), 268–298 (1996).
  19. M. Prabhu, N. S. Kim, and K. Ueda, "Simultaneous Double-Color Continuous Wave Raman Fiber Laser at 1239 nm and 1484 nm Using Phosphosilicate Fiber," *Opt. Rev.* **7**(4), 277–280 (2000).
- 

## 1. Introduction

Multi-wavelength fiber lasers have attracted considerable interest for their potential applications in optical communications, fiber sensors, optical instrumentation, and microwave photonic systems. Various gain approaches have been reported to achieve multi-wavelength lasing, including Erbium-doped fiber amplifier (EDFA) [1], semiconductor optical amplifier (SOA) [2], fiber Raman amplifier (FRA) [3]. It is well known that the intrinsic homogeneous line broadening and the cross-gain saturation characteristics of EDFAs make them unsuitable for attaining stable multi-wavelength lasing at room temperature when they are used in conjunction with a linear or ring laser cavity. SOA-based multi-wavelength fiber lasers are impractical because they cannot generate multiple-wavelengths with a high optical side-mode-suppression-ratio (SMSR). In addition, multiple wavelength lasers based on the use of Raman amplifiers are also impractical because they require several pump lasers of very high power levels. Recently, new approaches have been employed to realize multi-wavelength fiber lasers, such as the cooling of the EDF to 77 K by liquid nitrogen [4], the use of a frequency-shifted feedback technique within the laser cavities [5,6], the combination of different gain media within the same laser cavity [7,8], and the introduction of high nonlinearity or polarization hole burning elements into the laser cavity [9–12].

Single-wavelength tunable fiber lasers have been well developed and commercialized, and many demonstrations of multi-wavelength fiber lasers based on the use of different gain media within optical cavities have been reported [13,14]. However, the lasing wavelengths in such lasers are fixed. The ability to independently tune the wavelength in multi-wavelength fiber laser structures is vital for a large number of applications, such as fiber sensors, optical test instruments, and microwave photonic systems.

In this paper, we report a multi-wavelength tunable fiber laser based on the use of an Opto-VLSI processor in conjunction with erbium-doped optical amplifiers (EDFAs). The Opto-VLSI processor can arbitrarily select narrow wavebands from the amplified spontaneous emission (ASE) spectrum of the EDFAs and inject them into their corresponding fiber rings to generate laser signals simultaneously. The Opto-VLSI-based multi-wavelength tunable fiber laser can be electronically tuned within the gain bandwidth of the EDFAs, with a linewidth of less than 0.05 nm and a tuning step of 0.05 nm.

## 2. Opto-VLSI processor

An Opto-VLSI processor consists of an array of electro-optic cells independently addressed by a Very-Large-Scale-Integrated (VLSI) circuit to generate a reconfigurable, reflective digital holographic diffraction grating capable of steering and/or multicasting an optical beam [15]. It comprises a silicon substrate, evaporated aluminum, a quarter-wave plate (QWP), liquid crystal (LC), Indium-Tin Oxide (ITO) and a glass. ITO is used as the transparent electrode, and evaporated aluminum as the reflective electrode. The quarter-wave plate (QWP) layer between the liquid crystal and the VLSI backplane is responsible for polarization insensitivity, and polarization dependent loss for optical beam steering is as low as 0.5 dB [16]. The ITO layer is generally grounded and a voltage is applied at the reflective electrode by the VLSI circuit below the LC layer to generate digital phase holograms for optical beam control. Some

specific memory elements that store a digital voltage value are assigned to each pixel. This device is electronically controlled, software configurable, polarization independent, and very reliable since beam steering/multicasting is achieved with no mechanically moving part. The diffraction angle for the Opto-VLSI processor,  $\alpha_m$ , is given by:

$$\alpha_m = \arcsin\left(\frac{m\lambda}{d}\right) \quad (1)$$

where  $m$  is the diffracted order (in this paper only first order diffraction is considered),  $\lambda$  is the vacuum wavelength, and  $d$  is the grating period.

### 3. Structure of the Opto-VLSI-based multi-wavelength tunable fiber laser

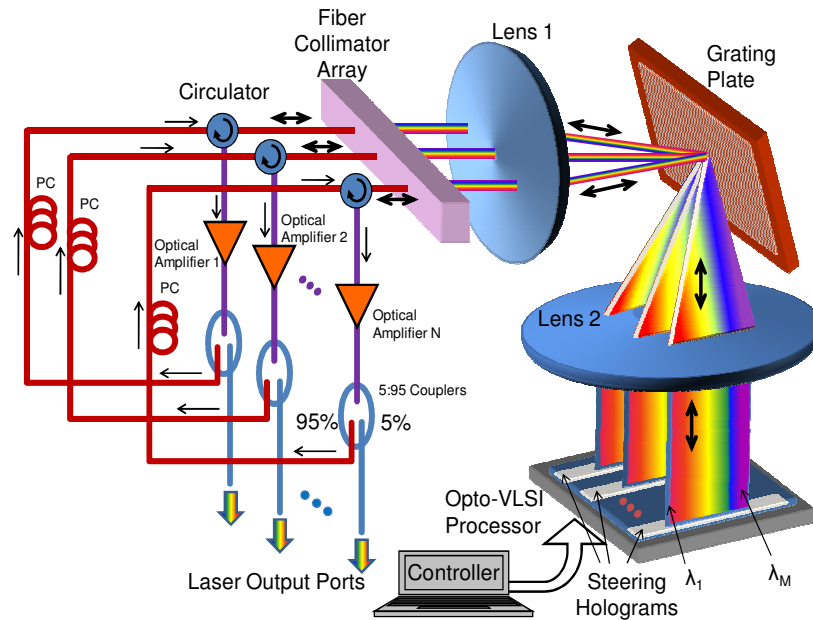


Fig. 1. The proposed multi-wavelength tunable fiber laser structure.

The proposed Opto-VLSI-based multi-wavelength tunable fiber ring laser structure is shown in Fig. 1. It consists of  $N$  tunable fiber lasers simultaneously driven by a single Opto-VLSI processor. Each tunable fiber laser employs an optical amplifier, an optical coupler, a polarization controller, a circulator, and one port from a collimator array. The broadband amplified spontaneous emission (ASE) noise from the gain medium is split by the optical coupler with a 5/95 power splitting ratio, where 5% of ASE power is used to extract the output of the tunable fiber laser while the remaining 95% is recirculated in the fiber ring cavity. The polarization controller (PC) is used to optimize the diffraction efficiency of the Opto-VLSI processor and to enforce single-polarization lasing. All the broadband ASE signals are directed to the corresponding collimator ports, via their corresponding circulators. A lens (Lens 1) is used between the collimator array and a diffraction grating plate to focus the collimated ASE beams onto a small spot onto the grating plate. The latter demultiplexes all the collimated ASE signals into wavebands (of different center wavelengths) along different directions. Another lens (Lens 2), located in the middle position between the grating plate and the Opto-VLSI processor, is used to collimate the dispersed optical beams in two dimensions and map them onto the surface of a 2-D Opto-VLSI processor, which is partitioned into  $N$  rectangular pixel blocks. Each pixel block is assigned to a tunable laser and

used to efficiently couple back any part of the ASE spectrum illuminating this pixel block along the incident path into the corresponding collimator port (according to Eq. (1)). The selected waveband coupled back into the fiber collimator port is then routed back to the gain medium via the corresponding circulator, thus an optical loop is formed for the single-mode laser generation. Therefore, by uploading the appropriate phase holograms (or blazed grating) that drive all the pixel blocks of the Opto-VLSI processor,  $N$  different wavelengths can independently be selected for lasing within the different fiber loops, thus realizing a multiport tunable fiber laser source that can simultaneously generate arbitrary wavelengths at its ports.

Note that this architecture offers excellent flexibility in terms of noninertial tuning because the lasing wavelengths can independently be selected using computer generated holograms.

#### 4. Experiments and results

To prove the principle of the proposed Opto-VLSI-based tunable fiber laser, an Opto-VLSI-based 3-wavelength tunable fiber laser was demonstrated using the experimental setup shown in Fig. 1. Each tunable fiber laser channel consists of an EDFA that operates in the C-band, a  $1 \times 2$  optical coupler with 5/95 power splitting ratio, and a fiber collimator array. A 256-phase-level two-dimensional Opto-VLSI processor having  $512 \times 512$  pixels with  $15 \mu\text{m}$  pixel size was used to independently and simultaneously select any part of the gain spectrum from each EDFA into the corresponding fiber ring. Two identical lenses of focal length 10 cm were placed at 10 cm from both sides of the grating plate. An optical spectrum analyzer with 0.01 nm resolution was used to monitor the 5% output port of each optical coupler which serves as the output port for each tunable laser channel. The 95% port of each ASE signal was directed to a PC and collimated at about 0.5 mm diameter. A blazed grating, having 1200 lines/mm and a blazed angle of  $70^\circ$  at 1530 nm, was used to demultiplex the three EDFA gain spectra, which were mapped onto the active window of the Opto-VLSI processor by Lens 2. A Labview software was specially developed to generate the optimized digital holograms that steer the desired waveband and couple back into the corresponding collimator for subsequent recirculation in the fiber loop.

The active window of the Opto-VLSI processor was divided into three pixel blocks corresponding to the positions of the three demultiplexed ASE signals, each pixel block dedicated for tuning the wavelength of a fiber laser. Optimized digital phase holograms were applied to the three pixel blocks, so that desired wavebands from the ASE spectra illuminating the Opto-VLSI processor could be selected and coupled back into their fiber rings, leading to simultaneous lasing at specific wavelengths. By changing the position of the phase hologram of each pixel block, the lasing wavelength for each fiber laser could be dynamically and independently tuned. The measured total cavity loss for each channel was around 12 dB, which mainly includes (i) the coupling loss of the associated collimator; (ii) the blazed grating loss; and (iii) the diffraction loss and insertion loss of the Opto-VLSI processor. Note that the total cavity loss influences both the laser output power and the tuning range, as well as the pump current thresholds needed for lasing (60mA in the experiments) [17].

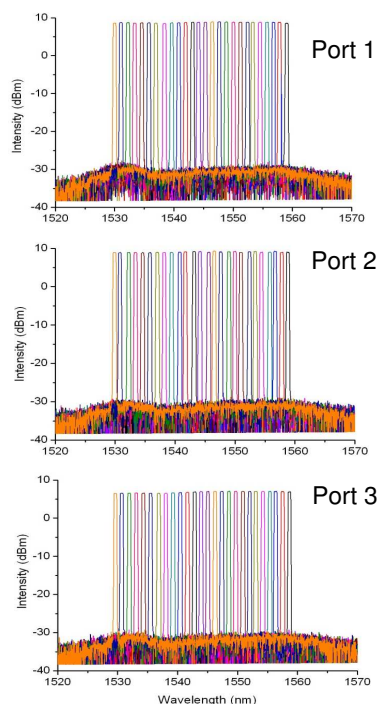


Fig. 2. Measured responses of the Opto-VLSI-based 3-wavelength fiber laser for coarse tuning operation over C-band. These three channels can independently and simultaneously be tuned over the whole C-band.

Figure 2 demonstrates the coarse tuning capability of the 3-wavelength Opto-VLSI fiber laser operating over C-band. The measured output laser spectrum for each channel is shown for different optimized phase holograms uploaded onto the Opto-VLSI processor. All the channels could independently and simultaneously be tuned over the whole C-band. Port 1 and Port 2 have an output power level of about 9 dBm with an optical side-mode-suppression-ratio of more than 35 dB. Port 3 has 2 dB less output power because the EDFA's gain for this channel was intentionally dropped to demonstrate the ability to change the output power level via changing the pump current. The laser output power for each channel has a uniformity of about 0.5 dB over the whole tuning range. Each laser channel exhibited very stable operation at room temperature when it was turned on for different periods of time ranging from a few hours to a few days. Figure 3 shows that the output power fluctuations at Port 2 are within 0.03 dB during an observation period of 1-hour for a lasing wavelength of 1550 nm.

The maximum output power for the multi-wavelength tunable fiber laser is about 9 dBm. This value is mainly dependent on the gain of the EDFA associated to that channel. Note that the thickness of the liquid crystal layer of the Opto-VLSI processor is very small (several microns), leading to spatial phase-modulation with negligible power loss. For high laser output power levels, the nonlinearity of the LC material could induce unequal phase shifts to the individual pixels of the steering phase hologram, leading to higher coupling loss, which reduces the output laser power. However, properly designed liquid-crystal mixtures can handle optical intensities as high as  $700 \text{ W/cm}^2$  with negligible nonlinear effects [18], making the maximum laser output power mainly dependent on the maximum output optical power of the gain medium.

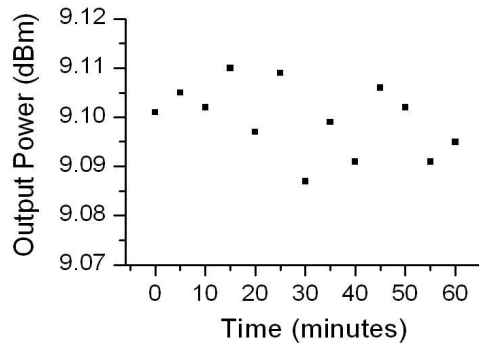


Fig. 3. The measured output power fluctuations at Port 2 for a lasing wavelength of 1550 nm.

The measured laser outputs for fine wavelength tuning operation of the three channels are shown in Fig. 4. By shifting the center of each phase hologram by a single pixel across the active window of the Opto-VLSI processor, the wavelength was tuned by a step of around 0.05 nm for all the three channels. This corresponds to the mapping of 30 nm ASE spectrum of the EDFA of each channel across the 512 pixels (each of 15  $\mu\text{m}$  size). Note that the tuning resolution can be made smaller than 0.05 nm by using an Opto-VLSI processor with a smaller pixel size. Note also that the shoulders on both sides of the laser spectrum of each tunable laser channel are due to self-phase modulation or other nonlinear phenomena arising from a high level of the output power [19].

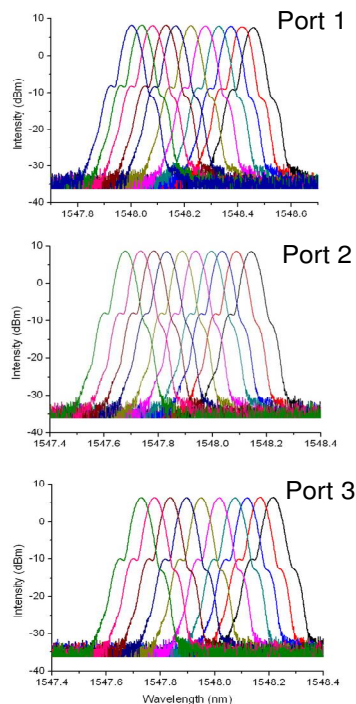


Fig. 4. Fine tuning operation for each channel of the Opto-VLSI-based 3-wavelength tunable fiber laser. The minimum tuning step was 0.05 nm.

Since the Opto-VLSI processor has a broad spectral bandwidth, the multi-wavelength tunable laser structure shown in Fig. 1 could in principle operate over the O-, S-, C- and/or L-bands. Note that when the output power of each fiber laser is varied via the control of the current driving the pump laser of the EDFA, the other laser characteristics such as output

SMSR, laser linewidth, output power uniformity, tuning step, and tuning range were not changed. The pump-independent laser linewidth observation might be due to the limited resolution (0.01 nm) of the OSA we used in the experiments. Note also that the Opto-VLSI processor used in the experiment was able to achieve wavelength tuning for up to 8 ports independently and simultaneously. This is because each pixel block was about 0.8 mm wide and the active window of the Opto-VLSI active window was 7.6 mm × 7.6 mm.

## 5. Conclusion

A novel multi-wavelength tunable fiber laser that uses an Opto-VLSI processor in conjunction with optical amplifiers has been proposed and demonstrated. A reconfigurable Opto-VLSI processor has been used to realize wavelength tuning through optical beam steering of ASE wavebands, and coupling them into the fiber laser cavities. Experimental results have demonstrated independent and simultaneous tuning of all lasing wavelengths over the entire C-band, and shown that the multi-wavelength tunable laser can achieve a high SMSR of more than 35dB, excellent tunability with a wavelength tuning resolution as small as 0.05 nm, a narrow linewidth of 0.05nm, a good power uniformity of 0.5 dB, and excellent stability at room temperature.